Macromolecular Symposia
www.ms-journal.de

Thermo-Mechanical Investigation on an Automotive Engine Encapsulation System Made of Fiberglass Reinforced Polyamide PA6 GF30 Material

Francesco Caputo, Giuseppe Lamanna, Alessandro De Luca, and Enrico Armentani*

This paper deals with technological solutions of innovative engine encapsulation systems for automotive. The aim of this device is to insulate acoustically and thermally the engine from the environment, in order to keep its temperature higher for more hours after it has been switched off. If the engine is subsequently started within this interval, the higher temperature involving the lubricating oil will allow reducing its viscosity, resulting in a lower level of energy dissipation due to friction losses, a lower fuel consumption and, consequently, a lower CO_2 emission level. In this paper, a finite element model is carried out in order to investigate on the thermo-mechanical behavior of the proposed engine encapsulation system.

1. Introduction

An important problem in engine design is that vehicle pollutant and noise emission limits will be reduced by the legislative authorities in the next few years.[1–3] Engine encapsulation systems offer the possibility of achieving these goals.[4,5] This paper deals with the design of an innovative engine encapsulation device for automotive, based on the use of composite materials. This technology consists in keeping the engine temperature higher for more hours after the engine has been switched off, so that, at the next start-up, the higher temperature will make the lubricating oil less viscous, providing benefits in terms of energy dissipation due to friction losses, fuel consumption, CO_2 emissions level, and acoustic insulation of the engine.[6]

In this paper, a first step has been dedicated to characterize experimentally the material properties of the fiberglass reinforced polyamide PA6 GF30 material of which the encapsulation system is mainly made. The need to use composite materials is due to the importance of keeping the automobiles weight low. Subsequently, material properties have been used for the development of the finite element (FE) model aimed to investigate on the thermo-structural behavior of the encapsulation system under critical loading conditions.[7,8] In detail, the engine cover has been studied assuming that it is subjected to an acceleration peak of 4 g (expected to affect the vehicle when it interacts with a bump in the road), under an engine temperature of 180 °C.

F. Caputo, G. Lamanna, A. De Luca
Department of Engineering
University of Campania "L. Vanvitelli,"
Via Roma 29, 81031 Aversa, Italy
E-mail: alessandro.deluca@unicampania.it
E. Armentani
Department of Chemical
Materials and Production Engineering
University of Naples Federico II
Corso Umberto I 40, 80138 Naples, Italy

DOI: 10.1002/masy.201900100

2. Test Article

Encapsulation (**Figure 1**) consists of a rock wool layer (in grey) aimed to reduce noise emissions and heat transfer with the environment; a movable component, made of PA6 GF30 material, covering the rock wool layer (in yellow) and a fixed PA6 GF30 component (in red). Yellow and red components are connected to each other by two hinges, allowing relative rotation.

3. Experimental Section

This section describes the PA6 GF30 material properties provided by the following experimental tests: tensile, flexural and creep tests. Tests were carried out at the Department of Engineering of the University of Campania "L. Vanvitelli."

3.1. Tensile Test

Specimens dimensions are detailed in **Table 1** with reference to **Figure 2**, where w_i and t_i are the width and the thickness measured at section $i = 1$, 2, and 3 of the specimens. Tensile tests have been performed by applying a quasi-static load by using an electromechanical test machine, Zwick/Roell 250, equipped with a 250 kN load cell. Tests were carried out in displacement control, at a crosshead speed of 1.25 mm min^{-1}, according to ASTM D638 standard.[9]

Material properties carried out by tensile tests are shown in **Table 2**.

According to **Figure 3**, the repeatability of the tests was demonstrated. Moreover, the three specimens showed a slightly off-center failure, as can be seen in **Figure 4**.

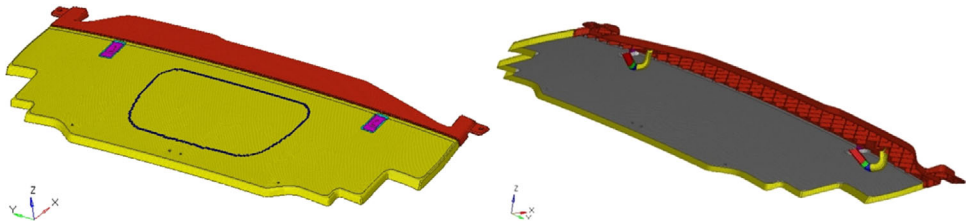

Figure 1. Engine encapsulation system.

Table 1. Specimen dimensions.

	L	L_0 [mm]	w_1 [mm]	t_1 [mm]	w_2 [mm]	t_2 [mm]	w_3 [mm]	t_3 [mm]
Sp. 1	150	57	9.4	3.85	9.4	3.85	9.45	3.85
Sp. 2	150	57	9.75	3.9	9.8	3.8	10	3.8
Sp. 3	150	57	9.8	3.8	9.75	3.9	9.75	3.9

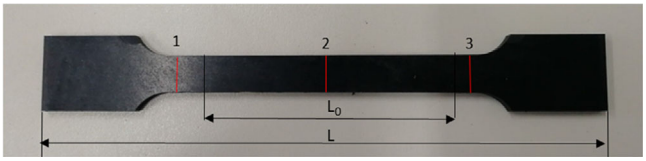

Figure 2. Specimen geometry.

3.2. Bending Test

Three-points bending test was carried out according to ASTM D790 standard.[10] Tests were carried out in displacement control, at a crosshead speed of 0.5 mm min^{-1}. Results, in terms of averaged force versus displacement curve, are provided in **Figure 5**.

Table 2. Material properties provided by the tensile tests.

	E [MPa]	σ_{sn} [MPa]	σ_f MPa]	ε_f [%]
Sp. 1	4601.13	73.43	90.00	4.36
Sp. 2	4385.05	72.37	91.17	3.92
Sp. 3	4224.94	70.69	89.57	4.56

E is the Young modulus, σ_{sn} is the Yield stress, and σ_f and ϵ_f are the stress and the strain at break. Figure 3 shows the stress–strain curves achieved by the tensile tests.

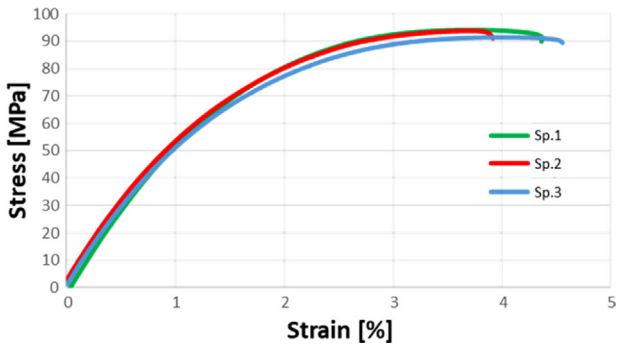

Figure 3. Tensile test.

According to the three-points bending test, Young modulus was assessed to be 4911.53 MPa, stress and strain at break, 80.06 MPa and 9.20%, respectively, and the maximum stress, 143.5 MPa.

3.3. Creep Test

A creep test was carried out according to ASTM 2990 standard.[11] The specimen was tested, in load control, under a tensile load, corresponding to a stress level of 60 MPa, at room temperature (23 °C), for 48 h. Strain versus time curve is shown in **Figure 6**.

4. FE Model

Finite element analysis has been carried out through Abaqus commercial code v. 6.14. The uncoupled approach[12,13] has been used in order to perform the thermo-mechanical simulation as well as to reduce the computational costs. Such an approach consists of two consecutive analyses: the former, performed by solving independently the thermal problem, allows achieving the temperature distribution by considering as starting condition an engine temperature of 180 °C; the latter considers the temperature distribution previously predicted as nodal thermal load. FE model consists of 194 104 nodes and 271 421 elements. With reference to Figure 1, brick elements, C3D4, C3D8, and C3D6 (from Abaqus elements library) have been used for the encapsulation component in red and for the rock wool layer in grey. Other parts have been modeled through shell elements, S4 and S3 (from Abaqus elements library). Relatively to PA6 GF30, material properties have been set according to the experimental tests previously described. For the car body (**Figure 7**), BH220 steel has been considered, while for the rock wool, a Young modulus of 20 MPa and a Poisson coefficient of 0.3 have been considered.

Concerning the boundary conditions, body car has been constrained symmetrically has shown in Figure 7a. In addition, the engine cover has been investigated under an acceleration of 4 g applied along the z-axis, as shown in Figure 7b. Engine cover has been constrained in correspondence of A point, simulating the clip aimed to avoid the relative rotation between the fixed and movable counterparts. Other joints have been modeled according to the techniques presented in refs. [14,15].

5. Results

Figure 8a shows the temperature distribution over the engine encapsulation system. Temperatures are shown in °C. Figure 8b

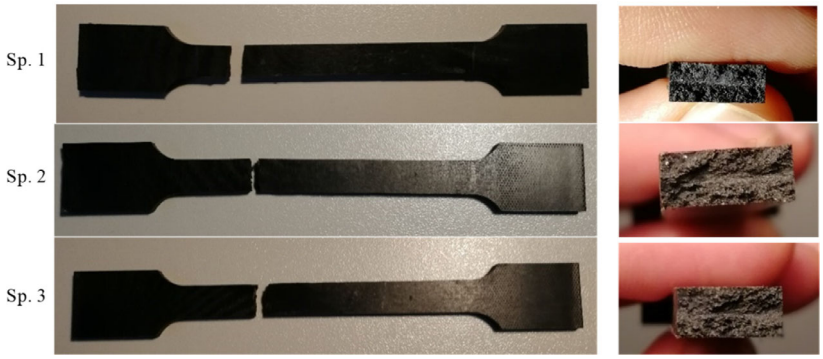

Figure 4. Specimens at break.

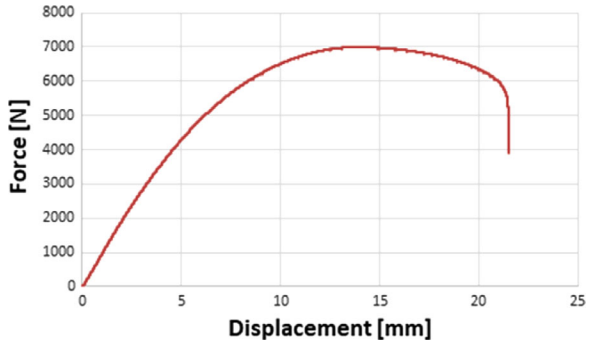

Figure 5. Force versus displacement curve provided by the bending test.

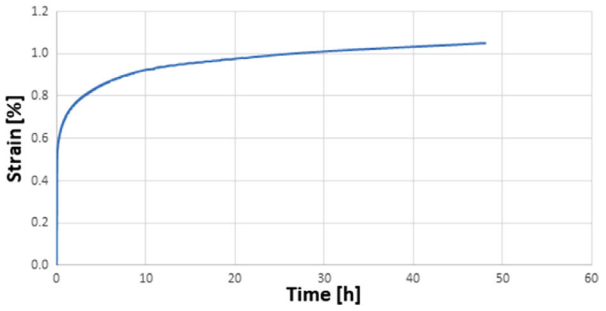

Figure 6. Strain versus time curve provided by creep test.

shows von Mises stresses map affecting the encapsulation system, achieved by considering the temperature distribution as nodal thermal loads for the mechanical analysis. According to Figure 8b, the maximum stress has been predicted to be 61.73 MPa and concentrated nearby the modeled clip (A point of Figure 7b).

Figure 9 shows the map of the nodal displacements along *z*-axis. The maximum displacement has been predicted to be 15 mm in the central part of the engine cover. Such a displacement may be too large leading it to touch the engine. Further investigation is needed.

6. Conclusions

In this paper, an innovative engine encapsulation system has been designed, aimed to reduce the CO_2 emissions. A thermo-structural analysis, based on the FE method, has been performed in order to investigate on the structural response of the proposed engine encapsulation system under critical loading conditions. In the analysis, the engine temperature has been supposed to be equal to 180 °C and the engine subjected to an acceleration peak of 4 g, representing the acceleration to which it is subjected when the vehicle interacts with a bump in the road surface. The analysis provided results consistent with expectations demonstrating the structural effectiveness of the designed encapsulation system.

Conflict of Interest

The authors declare no conflict of interest.

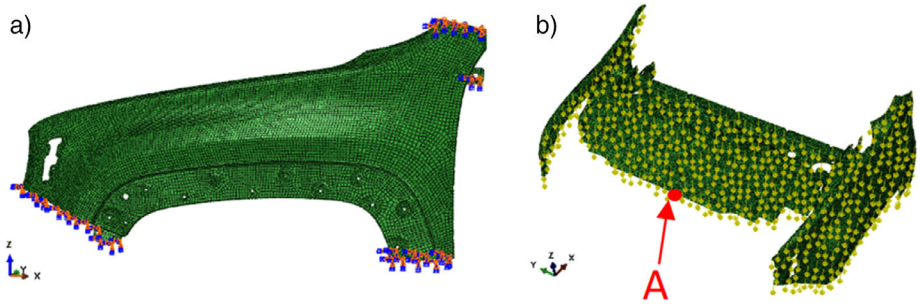

Figure 7. a) Constraints and b) loading conditions.

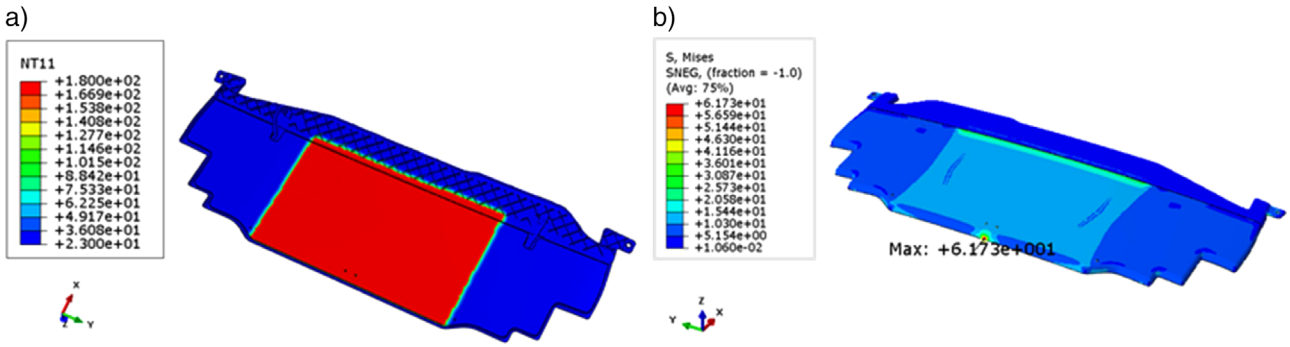

Figure 8. a) Temperatures distribution in °C and b) Von Mises stresses map in MPa.

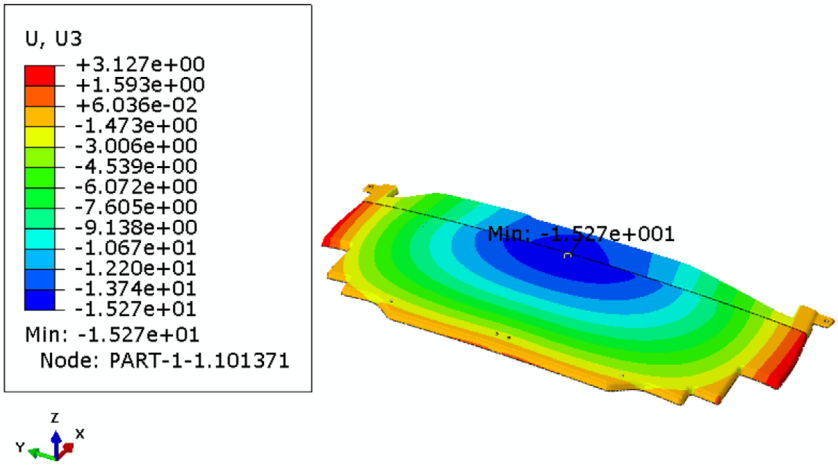

Figure 9. Displacements map in mm.

Keywords

engine encapsulation system, FEA, polymers material, thermo-structural analysis

[1] Regulation (EC) No 443/2009 of the European Parliament and of the Council of 23 April 2009 Setting Emission Performance Standards for New Passenger Cars as Part of the Community's Integrated Approach to Reduce CO_2 Emissions from Light-Duty Vehicles.
[2] A. Gruber, S. Bohlen, presented at ATZlive Automotive Acoustics Conf., Zurich, June **2013**.
[3] E. Bent, P. Shayler, A. La Rocca, presented at the Vehicle Thermal Management Systems Conf. Proc. (VTMS11), Coventry Technocentre, UK, May **2013**.
[4] F. Duvigneau, T. Luft, J. Hots, J. L. Verhey, H. Rottengruber, U. Gabbert, *Appl. Acoust.* **2016**, *102*, 79.
[5] D. Serban, G. Lamanna, C.G. Opran, *Proc. CIRP* **2019**, *81*, 677.
[6] T. Bürgin, presented at the Vehicle Thermal Management Systems Conf. Proc. (VTMS11), Coventry Technocentre, UK, May **2013**.
[7] F. Duvigneau, T. Luft, H. Rottengruber, U. Gabbert, presented at 21st Int. Congress on sound and vibration, Beijing, July **2014**.
[8] F. Duvigneau, S. Liefold, M. Höchstetter, J. L. Verhey, U. Gabbert, *J. Sound Vib.* **2016**, *366*, 544.
[9] ASTM D638-14, Standard Test Method for Tensile Properties of Plastics.
[10] ASTM D790-17, Standard Test Methods for Flexural Properties of Unreinforced and Reinforced Plastics and Electrical Insulating Materials.
[11] ASTM D2990-17, Standard Test Methods for Tensile, Compressive, and Flexural Creep and Creep-Rupture of Plastics.
[12] R. Sepe, M. Laiso, A. De Luca, F. Caputo, *Key Eng. Mater.* **2017**, *754*, 268.
[13] E. Armentani, A. Pozzi, R. Sepe, presented at *12th ESDA* Copenhagen, July 2014.
[14] F. Caputo, G. Lamanna, A. Soprano, *SDHM* **2011**, *7*.
[15] A. Riccio, F. Caputo, G. Di Felice, S. Saputo, C. Toscano, V. Lopresto, *Appl. Compos. Mat.* **2016**, *23*.